N91-24405

I. NATURAL AGING AND REVERSION BEHAVIOR OF Al-Cu-Li-Ag-Mg ALLOY WELDALITE™ 049

Frank W. Gayle, Frank H. Heubaum, and Joseph R. Pickens

The lattice images of T_1-like platelets in Weldalite™ 049 were compared with those in the literature for T_1 in other Al-Cu-Li alloys. From the [110] direction, the structures appear identical. However, when viewed from the [112] direction, the structures are different. Dozens of platelets were imaged from the [112] direction and, in each case, the structure was different from that reported for T_1 in the literature. The modified structure apparently results from the presence of Ag+Mg, but the reasons for the slight structural change as well as the details of the T_1 structure in Weldalite™ 049 are unknown.

1. INTRODUCTION

Recently an aluminum-copper-lithium alloy capable of 700 MPa yield strength in either the T8 or T6 temper has been developed [1,2]. In addition to such high strength levels, the Weldalite™ 049 alloy exhibits excellent properties in material aged at room temperature, both with (T3 temper) and without (T4 temper) prior cold work, and a strong reversion behavior when these "naturally aged" samples are heated to 160-180°C for short periods of time. The reverted temper is characterized by a reduced yield strength and increased ductility, which may be technologically useful, for example, in cold-forming operations.

The present study was initiated to understand the natural aging and reversion behavior of Weldalite™ 049 in tempers without cold work. Of particular interest are: 1) the microstructural basis for the high strength in the T4 condition, 2) an explanation of the reversion phenomenon, and 3) the effect of re-aging at room temperature after a reversion treatment. Mechanical properties were measured and transmission electron microscopy (TEM) analysis performed at various stages of microstructural development during aging, reversion, and subsequent re-aging.

2. EXPERIMENTAL PROCEDURE

Samples of Weldalite™ 049, nominally Al-6Cu-1.3Li-0.4Ag-0.4Mg-0.14Zr (wt.%), were obtained as extruded bar (19 x 51 mm) or rolled sheet (5 mm). Unless indicated otherwise, material was solution-heat-treated (SHT) at 503°C for 1 hour, quenched in cold water, and allowed to naturally age at room temperature. The naturally aged temper (T4) was defined as >1000 hours post-SHT. Samples of T4 were reverted at 180°C for periods from 5 to 45 minutes and subsequently "re-aged" at room temperature. Aging and re-aging behavior were followed by hardness (Rockwell B) and electrical conductivity measurements.

TEM specimens were prepared in a twin-jet polisher, using 25% HNO_3 in methanol. Polishing was performed at -25°C at ~12 volts. After polishing, it was necessary to dip the specimen in 50 vol.% HNO_3 in H_2O to remove Ag which had redeposited during electropolishing. Specimens were examined at an accelerating voltage of 120 keV using a Phillips EM400T transmission electron microscope.

3. RESULTS

The alloy displayed a rapid and strong natural aging response without prior cold work, as shown in Fig.1. Shown for comparison is the commercial Li-free alloy 2519 (Al-5.7Cu-0.2Mg-0.25Mn-0.1Zr-0.1V) in the form of 22-mm plate. After reversion, Weldalite™ 049 naturally ages with an incubation period that varies with reversion time as shown in Fig. 2. Note that room temperature re-aging eventually brings the reverted alloy back to the original T4 hardness. Tensile properties of the T4, reverted, and re-aged conditions (Table 1) correlate well with the hardness behavior of Fig. 2.

The microstructure of the T4 condition exhibits a very well developed Guinier-Preston (GP) zone [3,4] structure (Fig.3a). The zones, lying on {100} planes, are dense yet fairly fine (~5 nm diameter). The selected area diffraction pattern (SADP) shows streaking associated with the GP zone platelets (Fig.3b). Additionally, superlattice reflections are present for Al_3Li (δ'). Dark field imaging

TABLE 1. Longitudinal tensile properties of naturally aged and reverted Weldalite™ 049. (25 mm gauge; $\dot{\varepsilon} = 3 \times 10^{-4}$ s^{-1})

Aging Condition	0.2% YS MPa (ksi)	UTS MPa (ksi)	Elong. %
T4 (1000 h)	420 (61)	580 (84)	15.5
Reverted (180°C/15 min)	280 (40.5)	480 (69)	25.5
Reverted + 10^4 h re-age	440 (64)	610 (88.5)	11.0

of δ' indicates that the phase is generally uniformly distributed throughout the matrix, except for a preferred nucleation on the Zr-rich dispersoid known as α' or β'. This preferred nucleation is common in aluminum-base alloys containing both Li and Zr [5-7]. Thus the strong natural aging response of Weldalite™ 049 results from both GP zones and δ'.

The alloy after a 45 minute reversion was also characterized by TEM. After 24 hours re-age (i.e., before substantial re-aging takes

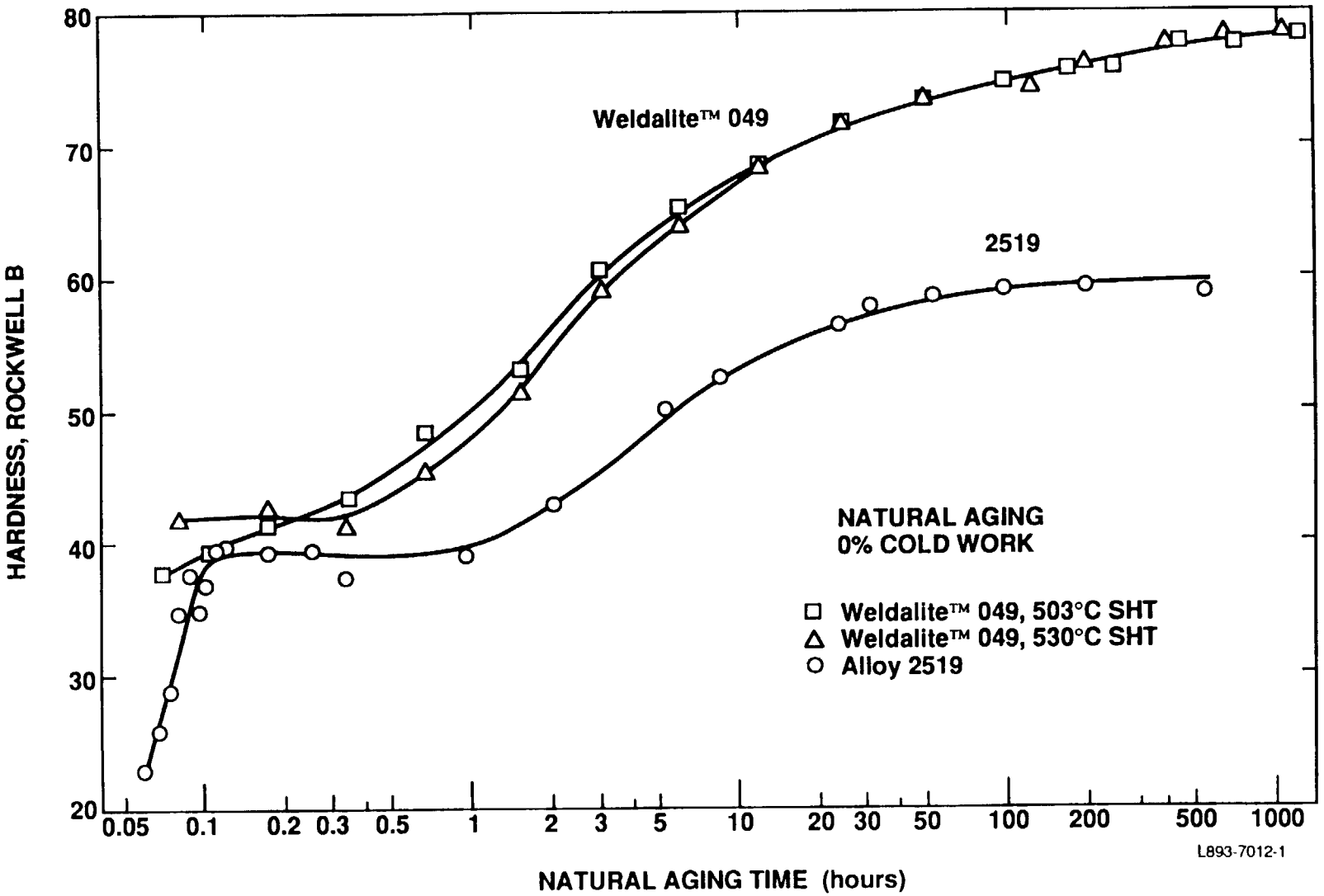

Figure 1 Natural aging curves for Weldalite™ 049 SHTed at 503°C and 530°C. Alloy 2519 is shown for comparison.

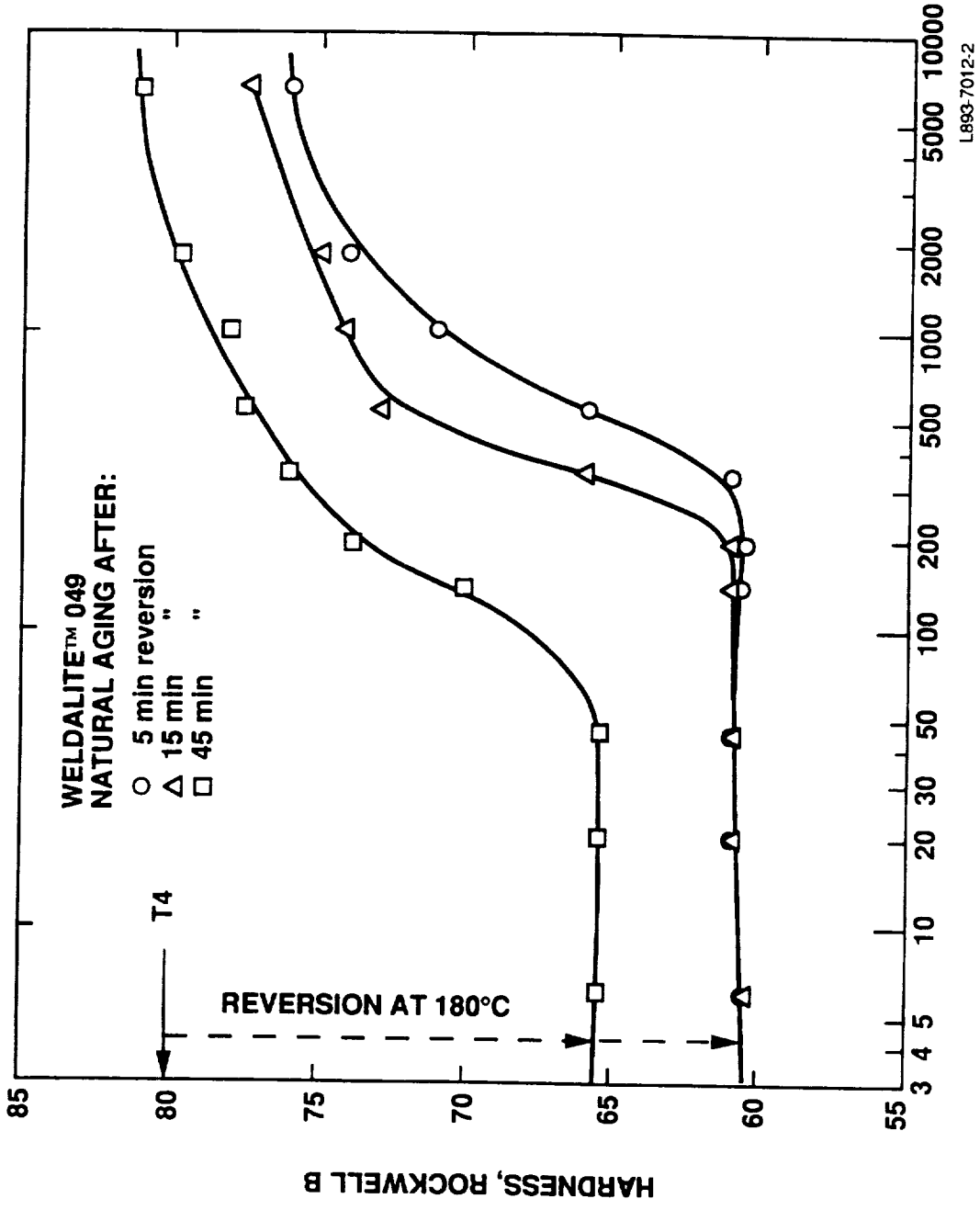

Figure 2 Natural aging response of Weldalite™ 049 after reversion at 180°C for 5, 15, and 45 minutes.

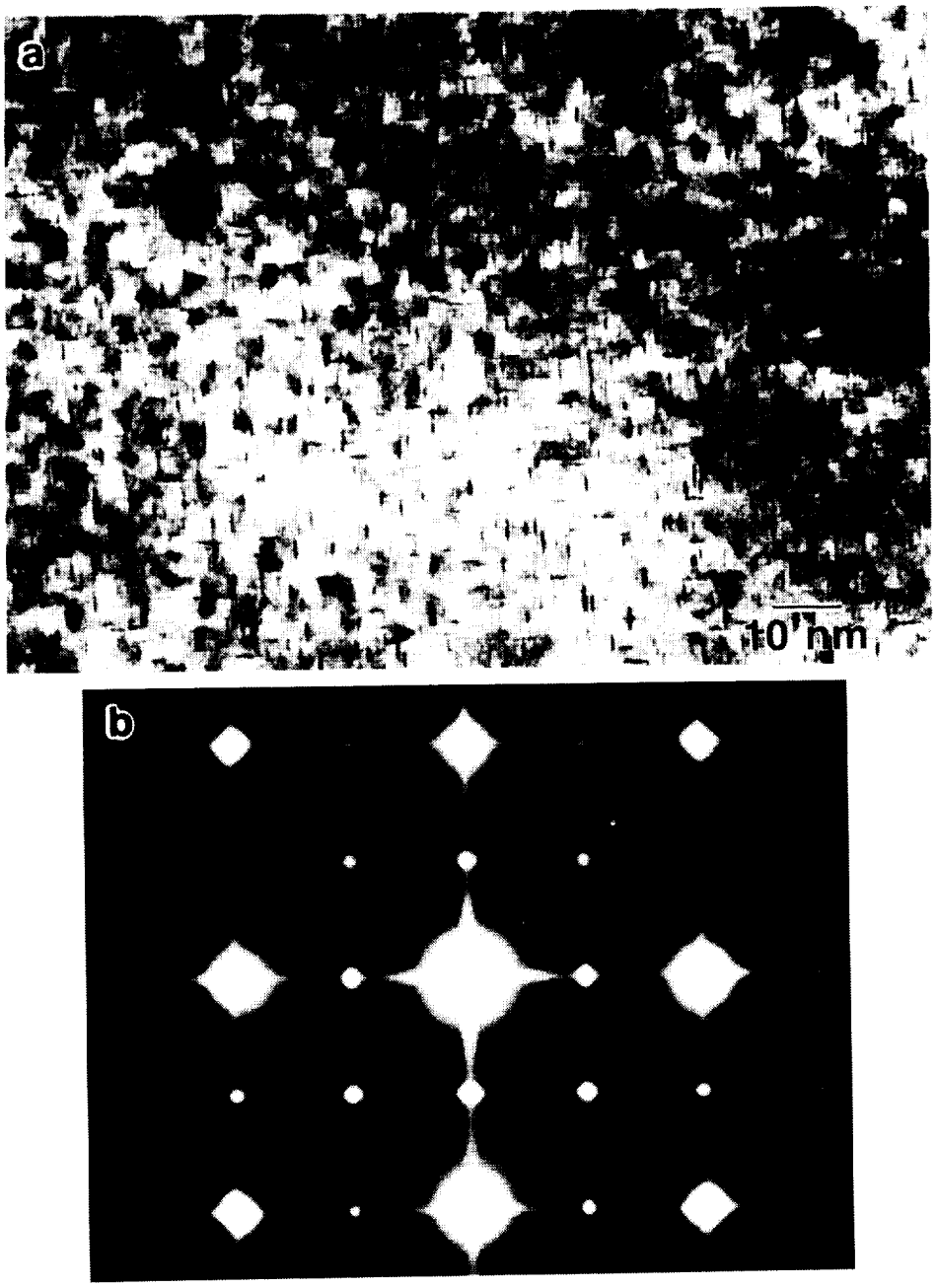

Figure 3 a) T4 microstructure consisting of fine but well-developed GP zones. The zones, lying on {100} matrix planes, are ~5 nm in diameter (TEM BF). b) B=001 selected area diffraction pattern which shows streaking associated with zones and superlattice reflections associated with δ'.

place), the structure reveals a coarser GP zone structure than for the T4 condition (Fig.4a). GP zones are now ~9-13 nm in diameter. The SADP contains continuous streaks without maxima, showing that the zones are still predominantly mono-layer GP1 zones. Multi-layered θ" (or GP2 zones), if present, would show streaks with intensity maxima developing at {100} locations [8]. The GP zones are homogeneously distributed, though the Zr-rich α' phase serves as a preferred nucleation site for the zones as well (arrow in Fig.4a). Additionally, the SADP gives little or no indication of superlattice reflections; thus the δ' has dissolved during reversion.

A 45 minute reversion sample was examined by TEM after 6400 hours of room temperature re-aging; at this point the material has regained its original T4 hardness. The structure contains a duplex GP zone population (Fig.5a), with larger zones (12-15 nm) resulting from growth of zones that were present after the reversion, and smaller zones (~2.5-5 nm) that nucleated during re-aging. Additionally, δ' revealed in a superlattice dark field image (Fig.5b) is present in at least three morphologies: 1) homogeneous, 1-2 nm spheres, 2) a coating on α' particles, and 3) a coating on the faces of the larger GP zones.

The SADP (Fig. 5c) is indicative of this complex structure. The continuous streaks are due to GP zones, and superlattice reflections from δ' are again present. Further, the superlattice reflections, both {100} and {110} type, are bi-directionally streaked due to the platelike morphology of δ' that occurs when coating the faces of GP zones.

4.0 DISCUSSION

The alloy under study has an extraordinary natural aging response with strengths similar to those of many aerospace alloys that are artificially aged to peak strength. The strength is due to a combination of fine GP zones and δ'.

The GP zone structure is developed far beyond that of other Al-Cu based alloys. For example, Wyss and Sanders [9] have studied alloys 2419 (Al-6Cu-0.3Mn) and 2519 (Al-6Cu-0.3Mn-0.2Mg) in the T4 temper and found little zone formation in the former and accelerated zone formation and concomitant strength enhancement in the latter. The Mg effect was suggested to be due to 1) enhanced diffusion associated with higher vacancy concentration when Mg is present, or 2) the

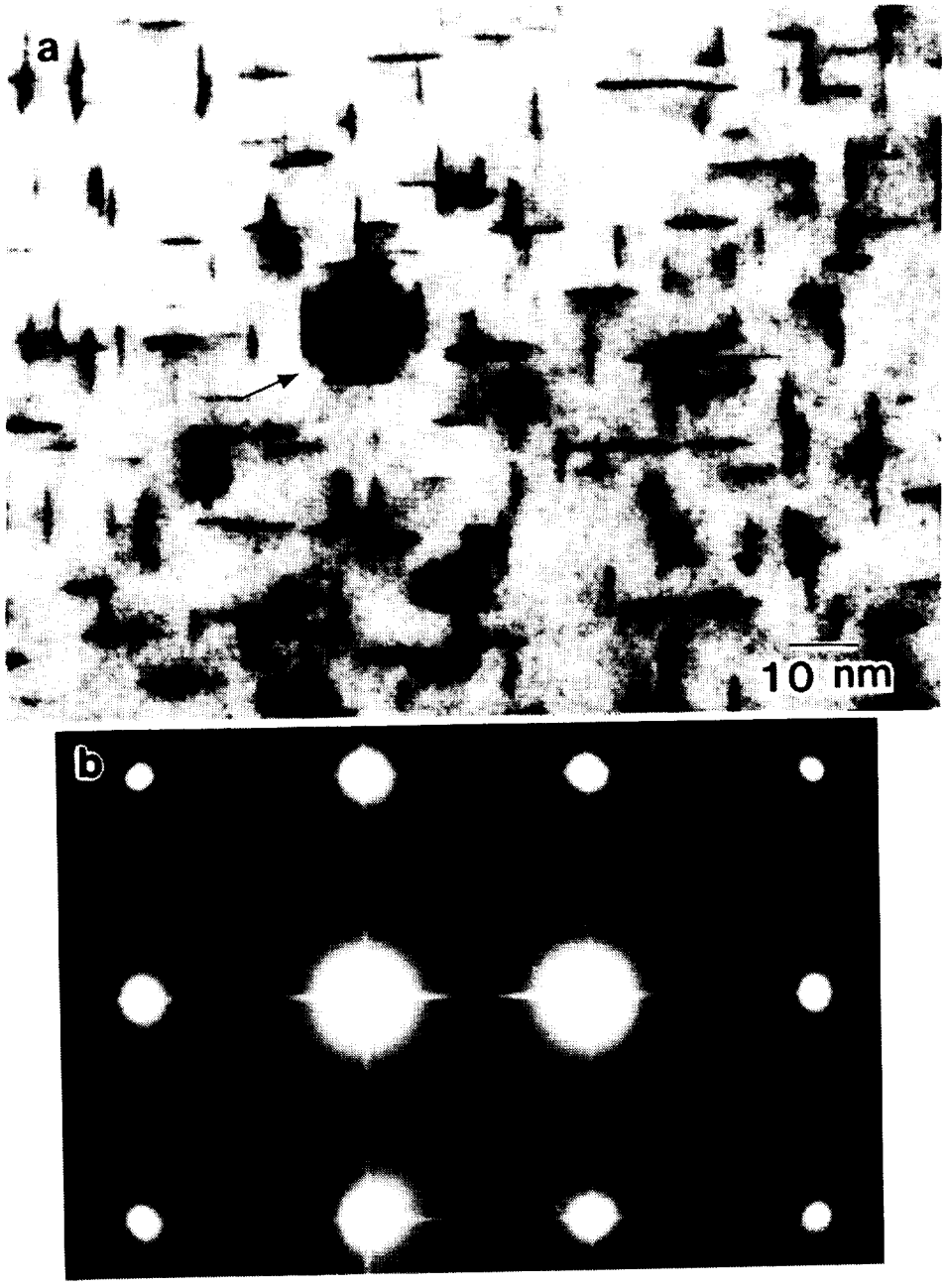

Figure 4 T4 temper, reverted 180°C/45 minutes and re-aged 24 h at room temperature (i.e., before significant re-aging has occurred). a) δ' has re-solutionized, leaving a coarser GP zone structure. Arrow indicates α' particle upon which GP zones heterogeneously nucleate. (TEM BF, B=001). b) Corresponding diffraction pattern containing continuous streaks and no δ' superlattice reflections.

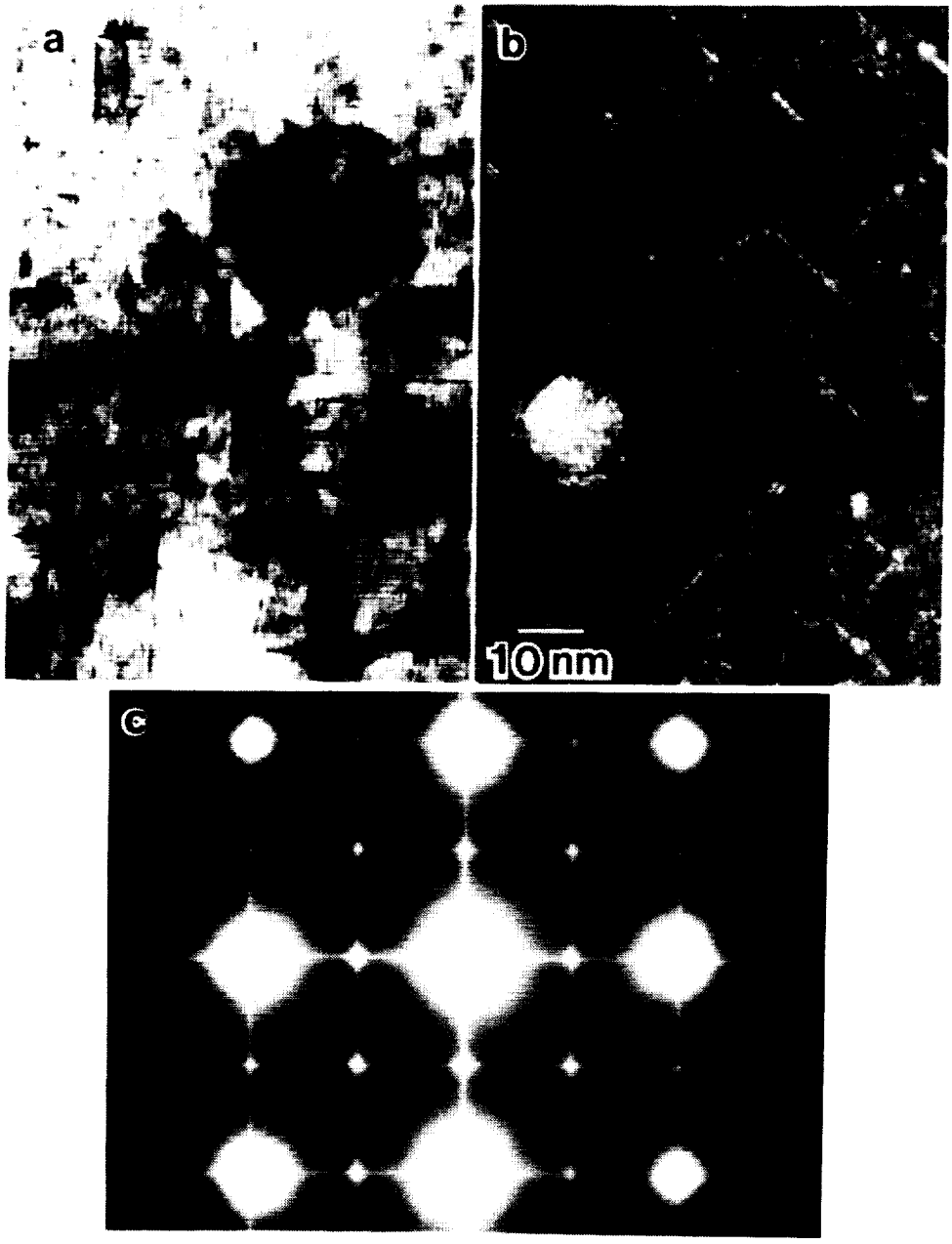

Figure 5 T4, reverted 180°C/45 min, re-aged 6400 h. at R.T. a) Two populations of GP zones, ~12-15 nm and 2.5-5 nm (BF TEM). b) g=110 dark field image showing δ' coating both sides of larger GP zones. δ' also appears as a coating on α' and as isolated 2nm spheres c) SADP shows streaking due to GP zones and superlattice spots due to δ'. Bi-directional streaking of the latter is due to plate-like nature of δ' on the faces of GP zones.

formation of Mg-vacancy complexes which serve as nucleation sites for GP zones.

In addition, Drits et al. [10] modified the Al-6.3Cu-0.3Mn Soviet alloy 1201 with minor Mg additions (0.05-0.12 wt.%) and observed dramatic increases in natural aging response. The standard 1201 alloy displayed a relatively small increase in yield strength of 19 MPa in 360 hours, whereas the alloy containing 0.12% Mg showed a rapid yield strength increase of 180 MPa in only 48 hours, and the strength was still increasing at 360 hours. The natural aging response increased monotonically with Mg content in the range studied. They explained the increase in strength by increased GP zone formation occurring at vacancy-impurity complexes, as previously proposed by Kelly and Nicholson [11]. Furthermore, Drits et al. imply that the high Mg-vacancy binding energy promotes the GP zone formation.

The present alloy exhibits far greater zone development than alloy 2519, based on both TEM images and streak development in SADPs. The Mg effect is likely similar to that observed in 2519 and Mg-bearing variants of alloy 1201. The contribution of Ag to this effect is being investigated in another study.

We propose a further effect to account for the rapid natural aging response -- a coupled growth of GP zones and δ'. The strain fields associated with each lead to a preferred juxtaposition of the two. In particular, δ,' which has a negative lattice misfit of ~0.08%, is favored in matrix compressive regions surrounding the perimeter of GP zones. Thus the energy barrier to nucleation associated with coherency strains (which are significant for coherent phases) would be reduced if the zones and δ' nucleated together or if either nucleated adjacent to the other. Preliminary dark field microscopy studies suggest the presence of such a relationship between δ' and zones of diameter <7 nm.

The reversion treatment lowers the yield strength by dissolving δ' and the fine GP zones. The coarser, lower density zone structure that remains is in a matrix with substantial Li and Cu supersaturation. With extended time at room temperature, fine GP zones and δ' re-precipitate, and original T4 strength returns, as shown in Table 1.

The microstructure after re-aging contains only two strengthening "phases", GP1 zones and δ', yet is quite complex. The GP zones, all on {100} planes, take three distributions with two major populations:

1) homogeneous zones, 12-15 nm } remaining after
2) zones nucleated on α', 12-15 nm } reversion
3) homogeneous zones, 2.5-5 nm, precipitated during re-aging.

The δ' phase, although present as a small volume fraction, also takes at least three distributions:

1) homogeneous, 1-2 nm spheres
2) heterogeneous envelopes on α'
3) face coatings on larger GP1 zones.

Additionally, there is preliminary evidence suggesting that δ' takes a fourth morphology, surrounding the perimeter of the small GP zones.

The long delay before significant re-aging occurs after reversion is surprising, considering the rapid aging response following SHT. Factors contributing to the long incubation are likely the annealing out of excess vacancies during the original aging and reversion treatments, and the solute depletion associated with the coarse GP zones after reversion. However, an understanding of the trends of incubation time with reversion duration time requires further investigation.

The observations in the present study of GP zone nucleation on α', and δ' nucleation on the faces of large GP1 zones adds to the already large number of configurations in which coherent phases can exist in Al-Li-Cu-Mg-Zr systems and subsystems. In each of these cases, one coherent phase serves as a heterogeneous nucleation site for another coherent phase (See Table 2). This behavior suggests new opportunities for strengthening and alloy design in Al-Li alloys.

TABLE 2. Coherent interfaces serving as nucleation sites for second coherent phases in Al-Li-Cu-Mg-Zr subsystems.

Nucleating Phase Desig.	Formula	Second Phase	Notes	Reference
α' or β'	$Al_3(Zr,Li)$	δ'	- - -	5-7
α' or β'	$Al_3(Zr,Li)$	GP1	P	- -
α' or β'	$Al_3(Zr,Li)$	θ'	- - -	12
α' or β'	$Al_3(Zr,Li)$	T_1	- - -	13
δ'	Al_3Li	T_1	A	14
θ'	Al_2Cu	δ'	- - -	12,15
GP1	(Cu)	δ'	P,B	- -
GP1 or θ'	- -	δ'	- - -	16

Notes: P - Present work

A - The nucleation of T_1 is proposed to occur within δ'.

B - Although GP1 zones are not considered to be a thermodynamically distinct phase, they effectively provide a coherent interface with the matrix.

5. SUMMARY

The Al-Cu-Li-Ag-Mg alloy known as Weldalite™ 049 exhibits remarkable strength following natural aging. This strength arises from a refined GP zone and δ' structure. Reversion at 180°C results in the dissolution of both δ' and some GP zones, leading to a lower number density of larger (~12 nm) GP1 zones. Re-aging at room temperature restores the original T4 strength, but only after an extended incubation period. The re-aged alloy is strengthened by GP zones and δ'. The structure is complicated, with the zones and δ' each occurring in at least three different morphological distributions, including new observations of the preferential nucleation of δ' on GP zones and GP zones on α'.

Acknowledgments. We thank R.K. Wyss of Alcoa for providing the 2519 plate. Some of the data included in this work were obtained under sponsorship of the National Institute For Standards and Technnology (NIST) and the Martin-Marietta Emerging Technology Program. The use of trade or brand names in the text does not imply endorsement of the products by NIST.

6. REFERENCES

[1] J.R. Pickens, F.H. Heubaum, L.S. Kramer, and K.S. Kumar, US Patent Application Serial No. 07/327,927 filed March 23, 1989, which is a continuation-in-part (CIP) of serial No. 083,333 filed August 10, 1987.

[2] J.R. Pickens, F.H. Heubaum, T.J. Langan, and L.S. Kramer, in "Aluminum-Lithium Alloys" (Proceedings of the Fifth International Aluminum-Lithium Conference), T.H. Sanders and E.A. Starke, eds., MCE Publications Ltd., Birmingham, U.K., 1989, p. 1397.

[3] A. Guinier, Ann.Physique 12, 1939, p.161.

[4] G.D. Preston, Proc.Roy.Soc.A 167, 1938, p.526.

[5] F.W. Gayle and J.B. VanderSande, Scr.Metall. 18, 1984, p.473.

[6] P.J. Gregson and H.M. Flower, J.Mat.Sci.Letters 3, 1984, p.829.

[7] F.W. Gayle and J.B. VanderSande, Acta Metall. 37, 1989, p.1033.

[8] V.A. Phillips, Acta Metall. 23, 1975, pp.751-767.

[9] R.K. Wyss and R.E. Sanders, Met.Trans.A 19A, 1988, pp.2523-2530.

[10] A.M. Drits, N.A. Vorob'yev, A.M. Zinden, O.I. Voroshilova, Russ. Metall. 4, 1981, pp. 142-145.

[11] A. Kelly and R. Nicholson, "Precipitation Hardening," Progress in Materials Science 10, pp. 149-392.

[12] M.H. Tosten, A.K. Vasudevan, and P.R. Howell, Aluminum-Lithium Alloys III (edited by C. Baker, et al., Institute of Metals, London, 1986), p.483.

[13] M.H. Tosten and P.R. Howell, Aluminum Alloys: Their Physical and Mechanical Properties (ed. by E.A.Starke and T.H.Sanders, EMAS, London, 1986), pp.727-741.

[14] V. Radmilovic and G. Thomas, J. Physique (Paris) 48, Colloque 3, 1987, p.C3-385.

[15] J.C. Huang and A.J. Ardell, Aluminum-Lithium Alloys III (edited by C. Baker, et al., Institute of Metals, London, 1986), p. 455.

[16] R. DeJesus and A.J. Ardell, in "Aluminum-Lithium Alloys" (Proceedings of the Fifth International Aluminum-Lithium Conference), T.H. Sanders and E.A. Starke, eds., MCE Publications Ltd., Birmingham, U.K., 1989, p. 1397.